AGU PUBLICATIONS

JGR

Journal of Geophysical Research: Solid Earth

RESEARCH ARTICLE
10.1002/2014JB011415

Key Points:
- Dense GPS network can be an independent tool to estimate water storage change
- Time-variable water mass change of dry and wet periods can be recovered by GPS
- GPS can fill missing water mass measurement and provide scaling factor for GRACE

Supporting Information:
- Figures S1–S3
- Movie S1
- Movie S2

Correspondence to:
Y. Fu,
Yuning.Fu@jpl.nasa.gov

Citation:
Fu, Y., D. F. Argus, and F. W. Landerer (2015), GPS as an independent measurement to estimate terrestrial water storage variations in Washington and Oregon, *J. Geophys. Res. Solid Earth*, *120*, 552–566, doi:10.1002/2014JB011415.

Received 24 JUN 2014
Accepted 5 DEC 2014
Accepted article online 9 DEC 2014
Published online 12 JAN 2015

GPS as an independent measurement to estimate terrestrial water storage variations in Washington and Oregon

Yuning Fu[1], Donald F. Argus[1], and Felix W. Landerer[1]

[1]Jet Propulsion Laboratory, California Institute of Technology, Pasadena, California, USA

Abstract The Global Positioning System (GPS) measures elastic ground loading deformation in response to hydrological mass variations on or near Earth's surface. We present a time series of change in terrestrial water storage as a function of position in Washington and Oregon estimated using GPS measurements of vertical displacement of Earth's surface. The distribution of water variation inferred from GPS is highly correlated with physiographic provinces: the seasonal water is mostly located in the mountain areas, such as the Cascade Range and Olympic Mountains, and is much smaller in the basin and valley areas of the Columbia Basin and Harney Basin. GPS is proven to be an independent measurement to distinguish between hydrological models. The drought period of 2008–2010 (maximum in 2010) and the recovery period of 2011–2012 in the Cascade Range are well recovered with GPS-determined time-variable monthly water mass series. The GPS-inferred water storage variation in the Cascade Range is consistent with that derived from JPL's GRACE monthly mass grid solutions. The percentage of RMS reduction is ~62% when we subtract GRACE water series from GPS-derived results. GPS-determined water storage variations can fill gaps in the current GRACE mission, also in the transition period from the current GRACE to the future GRACE Follow-on missions. We demonstrate that the GPS-inferred water storage variations can determine and verify local scaling factors for GRACE measurements; in the Cascade Range, the RMS reduction between GRACE series scaled by GPS and scaled by the hydrological model-based GRACE Tellus gain factors is up to 90.5%.

1. Introduction

Water resources for consumption and agricultural irrigation in the Western United States depend highly on precipitation of rain and snow during the fall and winter seasons. Monitoring and quantifying terrestrial water storage variations is therefore essential for practical applications, such as efficient water resource management and water-related policies. Observations from modern space-geodetic satellites have been widely applied to infer Earth's surface water variations. The Gravity Recovery and Climate Experiment (GRACE) measures large-scale hydrological surface mass change [*Tapley et al.*, 2004] at spatial resolutions of approximately 300 km and larger, limiting its application to these larger spatial scales. Hydrological assimilation models, such as the Global Land Data Assimilation System (GLDAS) [*Rodell et al.*, 2004], make use of water storage variations to constrain and optimize water cycle and storage simulations [*Zaitchik et al.*, 2008; *Houborg et al.*, 2012]. GRACE and GLDAS data are combined to study terrestrial water storage variations and groundwater changes [e.g., *Famiglietti et al.*, 2011]. Here, we use another space-geodetic tool, the Global Positioning System (GPS), to estimate terrestrial water mass variations in Washington and Oregon at monthly time scales from crustal loading deformation. The water thickness variations from the GPS network provide additional important information and increase spatial resolution over GRACE observations, and can be used as an independent verification tool for GRACE.

The paper is organized as follows: In section 2, we introduce continuous GPS measurements of vertical loading deformation in Washington and Oregon, and the inversion method used in this study. In section 3, we show GPS-determined water storage variations and compare with other independent observations, such as GRACE measurement, hydrological models, and in situ snow measurements. Additionally, we also demonstrate that GPS-inferred water series can be used as an independent tool to (1) fill temporal gaps when GRACE observations are missing, and (2) to determine local scaling factors for GRACE estimates. In section 4, we analyze advantages and disadvantages of GPS-inferred water variations, perform a series of synthetic tests and discuss potential errors in GPS time series. Finally, conclusions are summarized in section 5.

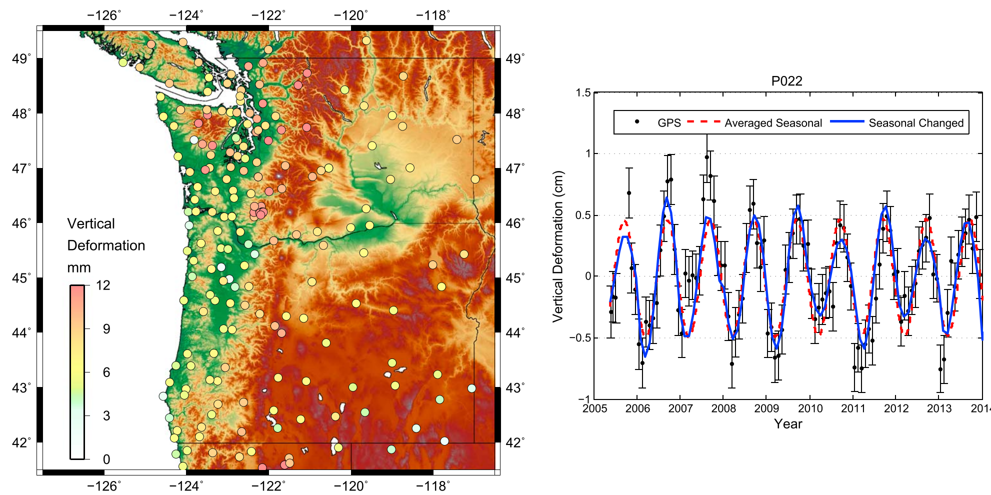

Figure 1. (left) Locations of continuous GPS stations used in this study. The color of circles shows GPS-measured multiyear averaged seasonal displacements. (right) A GPS monthly averaged detrended time series example of station P022, located in La Grande, Oregon. Both multiyear averaged seasonal variation and interannual variation are shown. The blue line is the time series fit whose seasonal terms change year by year. The seasonal range in deformation is defined as the position difference between 1 April (the end of winter) and 1 October (the end of summer).

2. Data and Methods

The Earth's crust is displaced in elastic response to a change in surface mass load [*Farrell*, 1972]. The Global Positioning System (GPS) accurately measures the crustal deformation at millimeter-level accuracy, having benefitted greatly from recent improvements of GPS processing strategies. GPS coordinates have been employed to investigate global [*Blewitt et al.*, 2001; *Wu et al.*, 2003; *Gross et al.*, 2004; *Tregoning et al.*, 2009] and local [*Heki*, 2004; *Grapenthin et al.*, 2006; *Fu and Freymueller,* 2012; *Fu et al.*, 2012a; *Ouellette et al.*, 2013; *Chanard et al.*, 2014; *Borsa et al.*, 2014; *Chew and Small*, 2014; *Amos et al.*, 2014] seasonal and long-term loading deformation modes. Studies also use GPS horizontal displacements to constrain the location of surface load changes [*Wahr et al.*, 2013], and compare with GRACE [*Fu et al.*, 2013].

GRACE observes monthly global mass redistributions at spatial scales of 300 km and larger. While the data record is largely continuous through 2010, several months of GRACE observations are missing since January 2011 due to the imposed active battery management (http://gracetellus.jpl.nasa.gov/data/GraceMonths/). There might also be a gap between the current GRACE mission and future GRACE Follow-on mission. We demonstrate how a dense GPS network can help to provide information about terrestrial water mass variations during missing GRACE months. In addition, we also determine the scaling factor for GRACE solutions based on GPS-determined water series to extend GPS's application for hydrological study as an independent measurement.

With a dense network, GPS has proven to be a high-resolution technique for evaluating seasonal water storage variability in California [*Argus et al.*, 2014]. In this study, we use the same inversion strategy based on elastic loading theory, a damped least square inversion method, to mainly investigate the yearly variability and long-term change in water storage variations in Washington and Oregon. In addition to the seasonal change, we also use GPS monthly time series to infer the time-varying monthly terrestrial water storage variation, an extension of previous study that only examined multiple-year averaged seasonal changes [*Argus et al.*, 2014].

2.1. Continuous GPS Measurements

We use JPL's GPS daily solutions in Precise Point Positioning mode [*Zumberge et al.*, 1997] processed with GIPSY software. JPL's reprocessed satellite orbits, clocks [*Desai et al.*, 2011] are based on absolute antenna phase center models for both satellite and receiver [*Schmid et al.*, 2007], and an improved solar radiation pressure model [*Sibthorpe et al.*, 2010]. The Vienna Mapping Function 1 (VMF1) [*Boehm et al.*, 2006; *Kouba*, 2008] is used, and ocean tidal loading is corrected with the FES2004 ocean tidal model [*Lyard et al.*, 2006] in a consistent reference

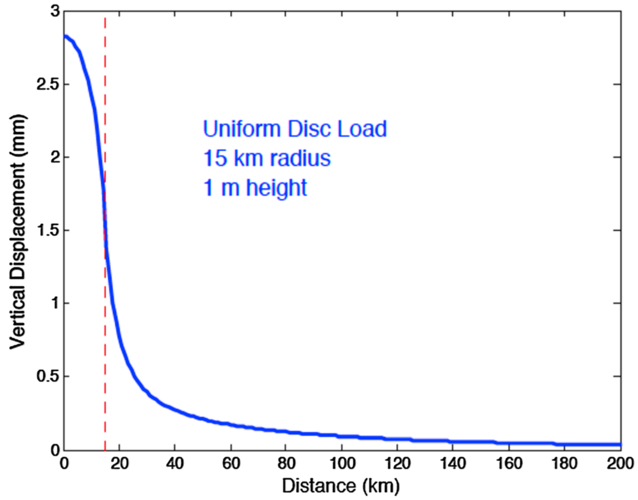

Figure 2. The vertical crustal displacement in elastic response to a removal of a uniform disk load with 1 m height and 15 km radius.

frame [*Fu et al.*, 2012b]. GPS positions are then transformed into the IGS08 reference frame, the IGS (International GNSS Service) realization of ITRF2008.

To study the loading deformation only due to hydrological near-surface water changes, we remove atmospheric loading effects from the GPS height estimates using the data and programs provided by the Global Geophysical Fluid Center (GGFC) [*van Dam and Wahr*, 1987; *van Dam*, 2010, http://geophy.uni.lu/ncep-loading.html]. The GGFC solution is 6 h, global surface displacement at 2.5° × 2.5° spacing determined from the NCEP (National Center for Environmental Protection) reanalysis surface pressure. We averaged atmospheric loading into daily and monthly corrections and removed them from GPS solutions as a postprocessed correction before the inversion for surface loads. This is effectively the same as applying the atmospheric loading correction at the observation level [*Tregoning and Watson*, 2009]. In Washington and Oregon, the atmospheric seasonal loading effect is small compared to the hydrological loading effects: the multiyear averaged seasonal vertical displacements due to atmospheric loading from April to October for the GPS stations in our study region are smaller than 1 mm [*van Dam*, 2010]. Therefore, the GPS-measured seasonal vertical ground oscillation in the study area is primarily caused by the hydrological loading effect.

Figure 1 (left) shows all the continuous GPS stations used in this study. The continuous GPS data span the period from 2006 to the end of 2013. To characterize GPS-measured crustal loading deformation, we perform three steps to derive and analyze the loading deformations from GPS time series:

1. We fit GPS time series with linear and annual terms and then determine a multiyear averaged (climatology) seasonal displacement. The seasonal range in deformation is defined as the position difference between 1 April (roughly the end of winter) and 1 October (roughly the end of summer). The GPS stations showing an elastic loading response to seasonal snow and rain subside from October to March during the main period of precipitation. The color of circles in Figure 1 (left) shows GPS-measured multiyear averaged seasonal displacements for all the stations used in this study.
2. We allow the seasonal annual terms to vary year by year and both amplitude and phase components are independently estimated, and can therefore evaluate the interannual variations. Figure 1 (right) shows an example of GPS station P022 located in La Grande, Oregon. The red dashed line denotes the multiyear averaged seasonal oscillation, and the blue line is the seasonal vertical deformation whose seasonal terms are estimated individually year by year, highlighting the interannual variations. The most apparent lower-than-average seasonal oscillation in the time series of P022 (blue line) occurs in 2010, which indicates a drought year.
3. We determine monthly averaged detrended GPS time series to remove potential long-term tectonic effect, and study the time-variable hydrological loading deformation in Washington and Oregon and invert for monthly terrestrial water mass change from the GPS time series.

2.2. Inversion Model

We follow the inversion method of *Argus et al.* [2014] and use Green's functions [*Wang et al.*, 2012] based on the PREM Earth model [*Dziewonski and Anderson,* 1981]. The vertical crustal displacement in elastic response to a removal of a uniform disk load with 1 m height and 15 km radius is shown in Figure 2. This can be considered as a forward model describing how the crust deforms as an elastic response to surface loading and unloading.

Our study aims to estimate terrestrial water variations based on GPS-measured loading deformation, which is an inverse problem. We adopt a damped least square inversion strategy to evaluate the optimal surface water mass variations from GPS-measured vertical loading deformation. This inversion strategy includes a bounded-variable least squares estimation strategy [*Stark and Parker*, 1995], and has been widely and successfully applied to slip estimations along seismogenic faults [*Harris and Segall*, 1987; *Price and Bürgmann,* 2002; *Hreinsdóttir et al.*, 2003; *Elliott et al.*, 2007; *Fu and Freymueller,* 2013].

We include the whole region of 39.5°N–51.5°N, Pacific coast-114.5°W for the inversion area, and divide this region into 0.25° × 0.25° patches. This region includes all of Washington and Oregon, and extends about 2.5° north into Canada, 2.5° south into California and Nevada, and 2.5° east into Idaho and Montana (note West is the Pacific Ocean); see the discussion for choosing this area to reduce inversion artifacts near the edges of inversion regions of Washington and Oregon.

In equation (1), the loading Green's functions (*G*) relate load mass variation at each patch and the vertical loading displacement at each GPS site (*b*). We apply smoothing constrains with a Laplacian operator (*L*) [*Harris and Segall*, 1987] to limit rapid and unrealistic water storage changes between neighboring patches. The inversion minimizes the combination of Weighted-Residual Sum of Squares (WRSS) and a roughness parameter as follows:

$$\underbrace{\|W(Gx-b)\|^2}_{\text{Misfit(WRSS)}} + \beta^2 \underbrace{\|Lx\|^2}_{\text{Roughness}} \rightarrow \min \tag{1}$$

in which β is a roughness weight and adjusts the relative weight between data fit (WRSS) and Roughness. We present details on how to choose a reasonable value for β in the discussion section later and conduct a series of synthetic tests for our inversion strategy.

3. Results

From GPS vertical position time series, we invert for three types of terrestrial water mass variations for Washington and Oregon: (1) multiyear averaged seasonal water change, (2) interannual variations, and (3) time-variable monthly terrestrial water variation history.

3.1. Seasonal Water Oscillations

The multiyear seasonal water storage changes in Washington and Oregon inverted from GPS have the largest amplitudes in the mountain regions: the Cascade Range, Olympic Mountains, and Blue Wallowa Mountains (Figure 3; the circles are GPS vertical seasonal displacements). In the valley and basin areas, such as Columbia Basin and Harney Basin, the seasonal water storage is much smaller. This result is consistent with the general pattern of seasonal water change in California [*Argus et al.*, 2014]. The pattern of seasonal water variation is strongly correlated with physiographic provinces (Figure 3), because total precipitation (both snow and rain) during fall and winter in the mountain regions is significantly larger than that in the valleys and basins. Additionally, high-elevation snow accumulation also results in relatively large surface loads.

The results thus far provide qualitative evidence that the dense GPS network in Washington and Oregon can accurately detect seasonal water loading variations between different physiographic provinces. We next compare our GPS-inferred seasonal water storage changes quantitatively to those simulated with hydrological models. We derived the total seasonal water storage from two hydrological models: (1) the North American Land Data Assimilation System (NLDAS-Noah) [*Mitchell et al.*, 2004] and (2) a composite model constructed from NLDAS-Noah soil moisture and snow water equivalent from the Snow Data Assimilation System (SNODAS) [*NOHRSC,* 2004].

Figure 4 shows the seasonal water storage change for Washington and Oregon from NLDAS and the composite NLDAS-Noah/SNODAS model. Figure 4 indicates that the composite model is close to the seasonal water inferred from GPS measurements (Figure 3), both in terms of magnitude and distribution. In contrast, the seasonal water storage changes from NLDAS are smaller by 30%–50% than those estimated from GPS. These results imply that NLDAS likely underestimates snowfall volume in Washington and Oregon, which is consistent with a similar conclusion for California [*Mitchell et al.*, 2004; *Argus et al.*, 2014].

10.1002/2014JB011415

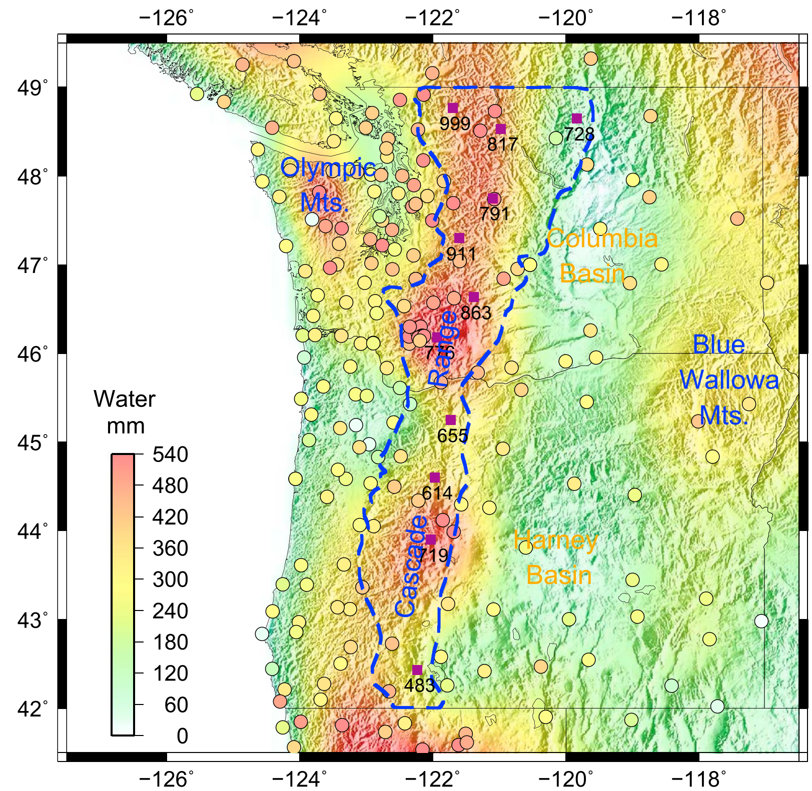

Figure 3. Seasonal water variations in Washington and Oregon inferred from GPS-measured multiyear averaged vertical seasonal loading deformation. The circles are GPS-measured seasonal displacements. Eleven purple squares show the locations of SNOTEL stations used for comparison in Figure 10, and three-digit numbers are their station names.

To characterize the multiyear averaged surface water loading variations from month to month, we also derive GPS monthly vertical loading deformations for each month, and then invert for monthly water storage change. An animation of the monthly surface water variations is included in the supporting information, and the snapshots for each month are also plotted in Figure S1 (supporting information). We use the surface water at the end of summer as a reference time and show how the water changes during a water year (from October to the end of September of the following year). The animation clearly demonstrates that GPS can

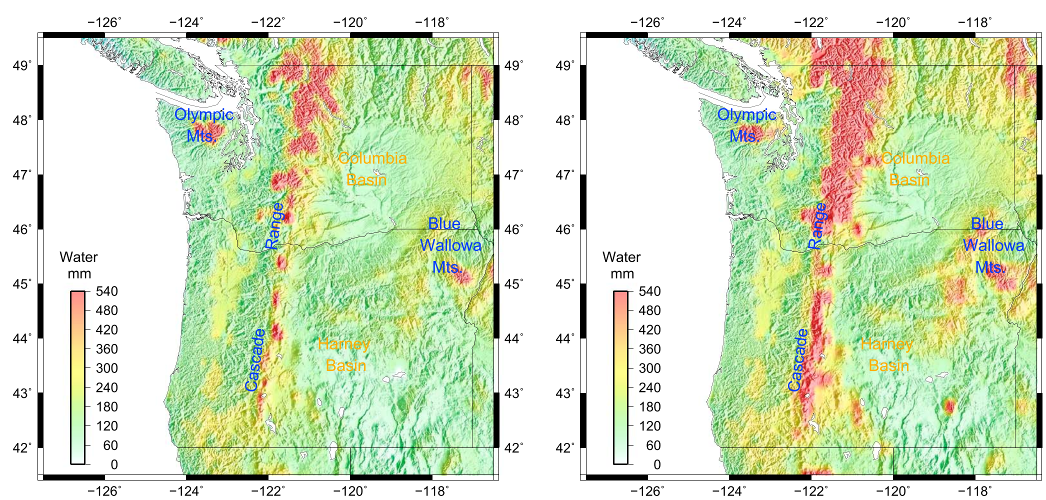

Figure 4. (left) Total seasonal water storage change from NLDAS-Noah model. (right) Total seasonal water storage from a composite model that combines NLDAS-Noah soil moisture and snow data from SNODAS.

10.1002/2014JB011415

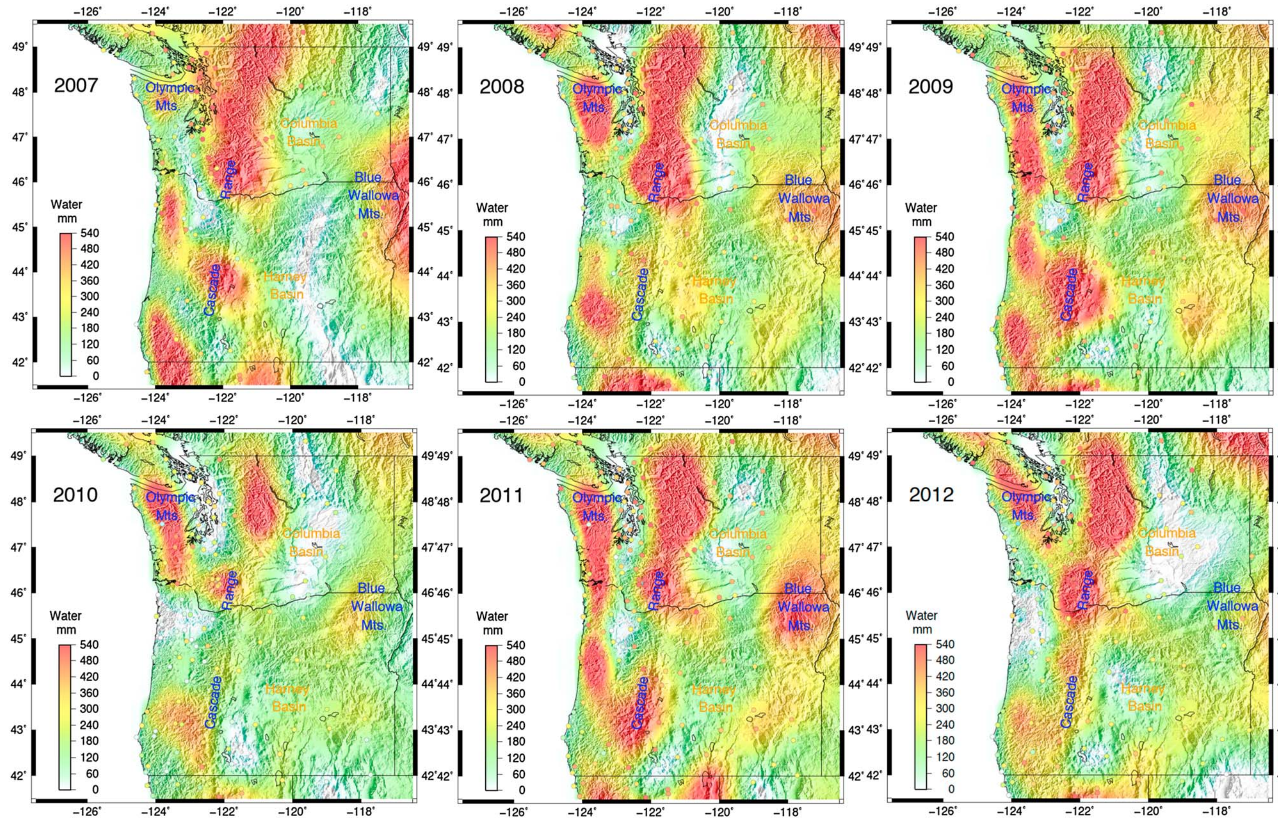

Figure 5. Seasonal water variations for individual years showing interannual variations, inferred from GPS-measured vertical seasonal loading deformation for each year (Figure 1, right).

accurately detect the water increase in Washington and Oregon that starts from October, reaches its maximum at the end of March, and returns to its minimum at the end of summer.

3.2. Interannual Variations

The GPS time series clearly show interannual variations (Figure 1, right) of the vertical ground seasonal oscillations within Washington and Oregon. Using GPS-measured seasonal vertical deformation estimated for different individual years, we next investigate the interannual variations of seasonal surface water storage.

Figure 5 compares the seasonal water storage variations in Washington and Oregon estimated each year from 2007 to 2012. The variations of terrestrial water mass from year to year are very clear. For example, the 2010 drought event is evident in contrast with other years (Figure 5) and the multiyear average (Figure 3). The quantitative comparison shows that the seasonal water oscillation in 2010 is ~65% of a normal year; also see the following results in section 3.3. The Washington state 2010 Legislature even prepared $4.2 million in dedicated funding for the 2010 drought response, and The Washington State Department of Ecology kept monitoring the event and published information online (http://www.ecy.wa.gov/drought/drtinfo.html). The drought event in 2010 led to less-than-average annual seasonal water in Washington and Oregon, and accordingly, GPS stations observed smaller crustal seasonal displacements (Figures 1 and 5) during this year. An animation comparing the interannual variations from 2007 to 2012 is included in the supporting information.

3.3. Time-Variable Water Storage Variations

To investigate the terrestrial water variations at higher temporal resolution, we use monthly averaged detrended GPS height time series to invert for time-variable water load changes in Washington and Oregon, and show the water variation history within the mountain system in these two states. We use GPS time series from 2006 onward because the major part of PBO (Plate Boundary Observatory) stations was established at that time.

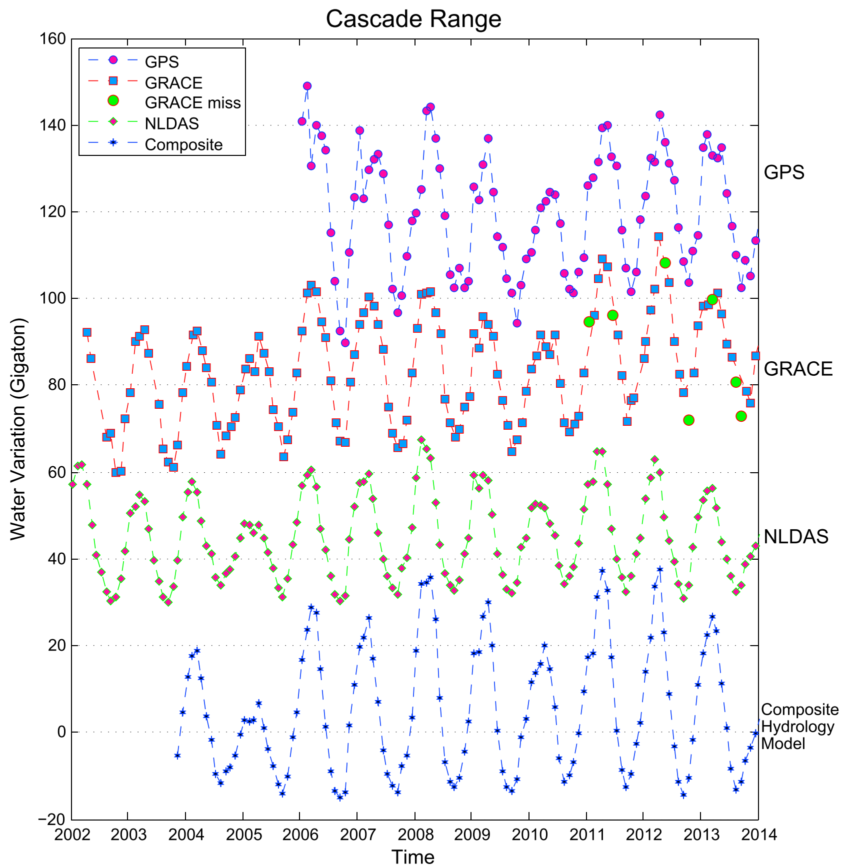

Figure 6. Water storage variations within the Cascade Range in Washington and Oregon inferred from GPS monthly time series, and comparisons with GRACE, NLDAS, and our composite hydrological models. Solid green circles are water storage change values filled for GRACE solutions with GPS inversion results, for the months that GRACE measurements are not available.

3.3.1. GPS-Inferred Result

Figure 6 shows monthly terrestrial water mass variations in the Cascade Range of Washington and Oregon inferred from GPS monthly time series, and comparisons with JPL's GRACE monthly mass grid solutions, as well as the NLDAS and composite hydrological models. JPL's GRACE solutions can be downloaded from the GRACE Tellus website (http://grace.jpl.nasa.gov), and details of the data processing algorithms are described in *Swenson and Wahr* [2006] and *Landerer and Swenson* [2012]. The area of the Cascade Range is outlined with blue dashed lines in Figure 3.

In the Cascade Mountains, GPS-inferred surface water change clearly shows the drought period from 2008 to 2010 with decreasing terrestrial water storage. The drought reached its maximum in 2010, and the seasonal water cycle in 2010 is only ~65% of a normal year. GPS, GRACE, and hydrology models all clearly record this drought year of 2010. From 2011 to the end of 2012, the terrestrial water storage in the Cascade Range has slightly increased as inferred from GPS, which is consistent with GRACE and the hydrological models. This demonstrates that GPS is an independent means to monitor and estimate time-variable water storage variations in Washington and Oregon.

We also divide the Cascade Range into Washington and Oregon parts and compare for water storage variation differences between these two states. GPS inversion results (Figure 7) indicate that the water storage variation in Washington is larger than that in Oregon, and this is consistent with GRACE solutions and hydrological models. Quantitative comparison indicates that the seasonal water storage change in Oregon is about ~45%–65% of that in Washington. While the time-variable water storage trend variations are similar between these two states, GPS results show some differences between Washington and Oregon. For example, the water variation of Washington in 2012 is much larger than other years, but the water change of

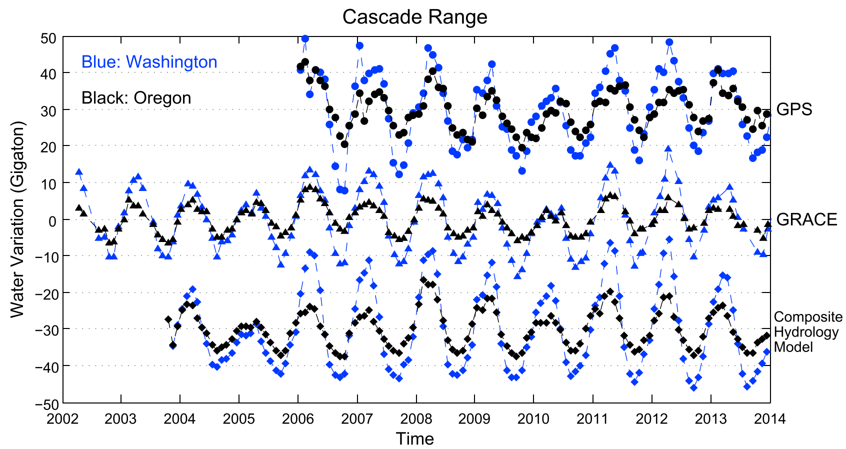

Figure 7. Comparison of water storage variations for the Cascade Range in Washington and Oregon. Blue is monthly water storage change of the Cascade Range in Washington, and Black is the result for the Cascade Range in Oregon.

Oregon in 2012 is smaller than that of 2011, and this is also true from GRACE and hydrological models, which indicate that GPS-determined water variations can distinguish water storage variations between regions.

To compare the differences of water storage between GPS inversion result, GRACE measurement, and hydrology models, we derive the series of difference between GPS inversion result and GRACE measurements (red dots, Figure 8), GPS inversion result and NLDAS hydrology model (blue triangles, Figure 8), and GPS result and the composite hydrological model (green diamonds, Figure 8). To quantify the consistency between GPS and other measurements, we use the percentage of RMS Reduction for comparison [*van Dam et al.*, 2007; *Tregoning et al.*, 2009; *Fu and Freymueller*, 2012]. For example, to compare GPS with GRACE, we remove GRACE water variations from GPS-inferred water change series and then calculate the reduction of RMS using the following equation:

$$\mathrm{RMS}_{\mathrm{Reduction}} = \frac{\mathrm{RMS}_{\mathrm{GPS}} - \mathrm{RMS}_{\mathrm{GPS\text{-}GRACE}}}{\mathrm{RMS}_{\mathrm{GPS}}} \qquad (2)$$

The percentage of RMS reduction between GPS and GRACE is 62.3%, between GPS and NLDAS 35.6%, and between GPS and the composite hydrology model 39.5%. The quantitative comparison yields larger differences between GPS and hydrological models than between GPS and GRACE. Differences between GPS, GRACE, and the hydrological models used in this study may arise due to completely different data acquisition methods and the implied sampling and process-representations. For example, GRACE is sensitive to long-wavelength surface load change. Hydrology models, both in assimilating and nonassimilating modes, highly depend on the quantity and quality of meteorological forcing data and observations (e.g., precipitation). Our GPS inversion strategy may smooth out some fine-scale local features where we do not have dense enough measurements to adequately constrain the surface load changes. However, the closer agreement between GRACE and GPS indicates that terrestrial water storage variations observed by these

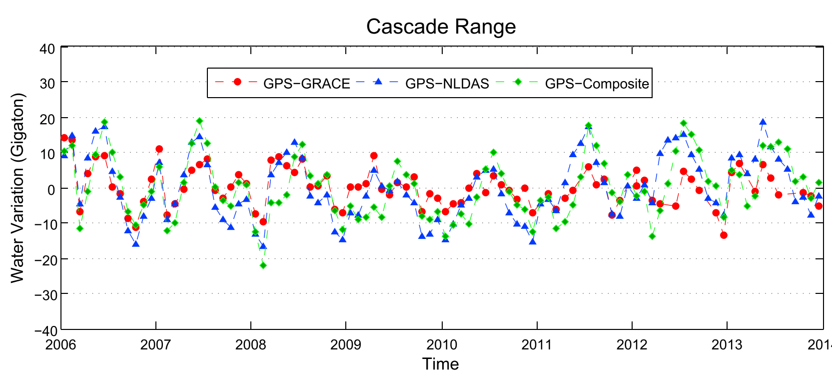

Figure 8. The differences between GPS-determined water storage variations, GRACE measurements, and hydrological models.

methods is more accurate than that simulated by models. Whether this is due to missing model physics or parameterizations or deficiencies in the models' forcing data will need to be resolved in future studies.

3.3.2. Fill GRACE Missing Periods With GPS Results

Because of active battery management on one of the GRACE satellites, there are several months when gravity observations are not available (as of the end of 2013: January, June 2011, May, October 2012, March, August, September 2013). In Figure 6, we highlight these months and fill the water storage change values for GRACE solutions for these months with GPS inversion results. For those months with missing GRACE measurements, we first use GPS-determined water series to calculate the relative water mass change of those months with their neighboring months, and use these information to interpolate the values for these months with GRACE observations are missing (solid green circles in Figure 6). This can be an important application of GPS-determined water change to fill the temporal gaps of current GRACE mission. More importantly, there might also be a period between the current GRACE mission and the future GRACE Follow-on mission without GRACE observation, and GPS can provide observations to monitor water storage change during this period.

For the months when GRACE measurements are missing, a simple way to estimate mass change is a linear interpolation using GRACE data of neighboring months, but this interpolation may lead to incorrect estimates. For example, for January 2011, both GPS and hydrological models indicate that the water storage value of January 2011 is closer to that of February 2011 (Figure 6). An interpolation with only GRACE measurements at neighboring months would give an incorrectly smaller water storage value than interpolated with GPS (Figure 6). This indicates that GPS provides independent information to correctly fill water storage values for the months when GRACE observations are missing. Additionally, the October 2012 GRACE measurement is not available, but this is the time where water storage is minimum in 2012. Direct linear interpolation only using GRACE data would miss this "trough" value and provide a wrong seasonal peak estimate. With the GPS-derived independent water change values, we correctly recover water storage at this important time where water changes reach their seasonal extreme. Those results demonstrate that GPS can be an independent measurement to provide water resource estimations for the regions with dense GPS networks, and fill the current and potential future temporal gaps when GRACE measurements might not be available.

3.3.3. Determination of Local Scaling Factor for GRACE From GPS

GRACE observations require the application of postprocessing filters that aim at reducing systematic errors, but some true geophysical signals are also damped. To compensate these effects, a gain factor from an independent hydrology model is usually applied [*Landerer and Swenson*, 2012]. Using the GPS-derived surface water storage variations, we can also determine the scaling factor for GRACE solution by minimizing the difference between GPS-derived water series and GRACE water series. Figure 9 compares water storage change in the Cascade Range (Figure 3) from GPS inversion result, GRACE original solution without scaling, GRACE measurements scaled with gain factors from the GRACE Tellus website (http://grace.jpl.nasa.gov) [*Landerer and Swenson*, 2012], and GRACE measurements scaled with GPS-inferred water change series. The results show that the scaled GRACE solutions with GPS data are consistent with the solutions scaled with the hydrological model-based gain factors by *Landerer and Swenson* [2012]. We also compute the RMS Reduction between GPS and GRACE using equation (2) to quantitatively assess their consistency. The percentage of RMS reduction between GRACE water series scaled by GPS (black line in Figure 9) and scaled by *Landerer and Swenson* [2012] with the hydrological model-based factors (blue lines in Figure 9) is up to 90.5%. This confirms that GPS can also provide accurate scaling factor to GRACE solutions as an independent measurements for the areas with dense GPS network.

3.3.4. Comparison With In Situ Snow Measurements

Obtaining ground truth total water storage estimates over spatial scales covered by GPS (or GRACE) is very difficult. We nevertheless compare our GPS-inferred surface mass change with in situ snow water equivalent changes in the Cascade Range, where snow volume change is a significant source of surface load variations. We use the Snow Water Equivalent (SWE) measurements provided by SNOTEL (short for Snow Telemetry, maintained by the National Water and Climate Center, http://www.wcc.nrcs.usda.gov/snow/) for our comparison. Figure 10 (left) shows SWE time series for the 11 SNOTEL stations selected for this study within the mountain area and the corresponding time-variable mass change derived from GPS. The locations of these 11 sites and their station names (three-digit number) are plotted in Figure 3. As an example, for SNOTEL site 863, which is located in White Pass, Washington, both SNOTEL and GPS indicate that surface mass reduced from 2008

10.1002/2014JB011415

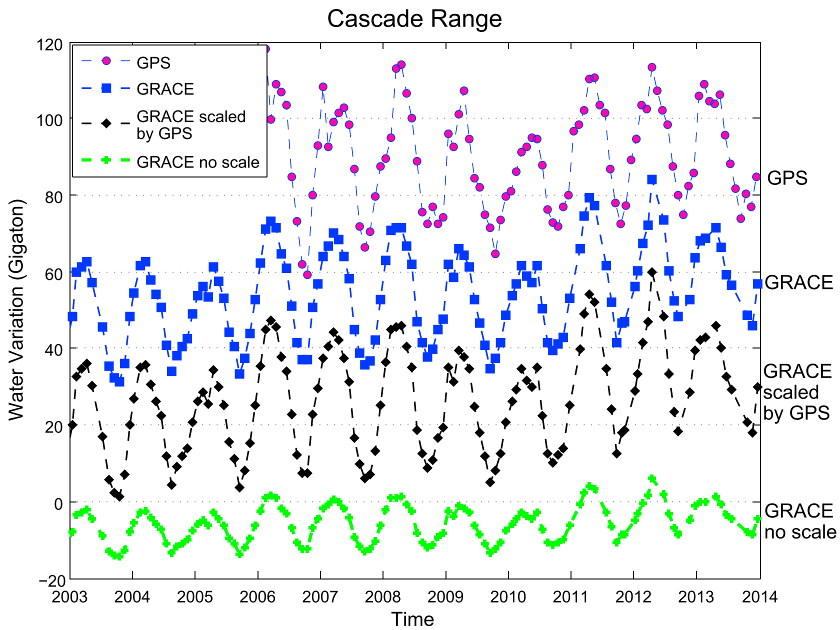

Figure 9. Demonstration of using GPS-inferred water variation to determine scaling factors for GRACE. GPS, GPS inversion result; GRACE no scale, GRACE original solution without scaling; GRACE, GRACE measurements scaled with gain factors from the GRACE Tellus website (http://grace.jpl.nasa.gov) [*Landerer and Swenson*, 2012], and GRACE scaled by GPS, GRACE measurements scaled with GPS-determined water change series.

to 2010 and increased from 2011 to 2012. The similar agreements of water change patterns can also be found for SNOTEL site 776 (Spencer Meadow, WA) and site 817 (Thunder Basin, WA). Figure 10 shows that GPS-inverted water variations are smoother than SNOTEL measurements, and this is due to the smoothing process inherent in the GPS inversion.

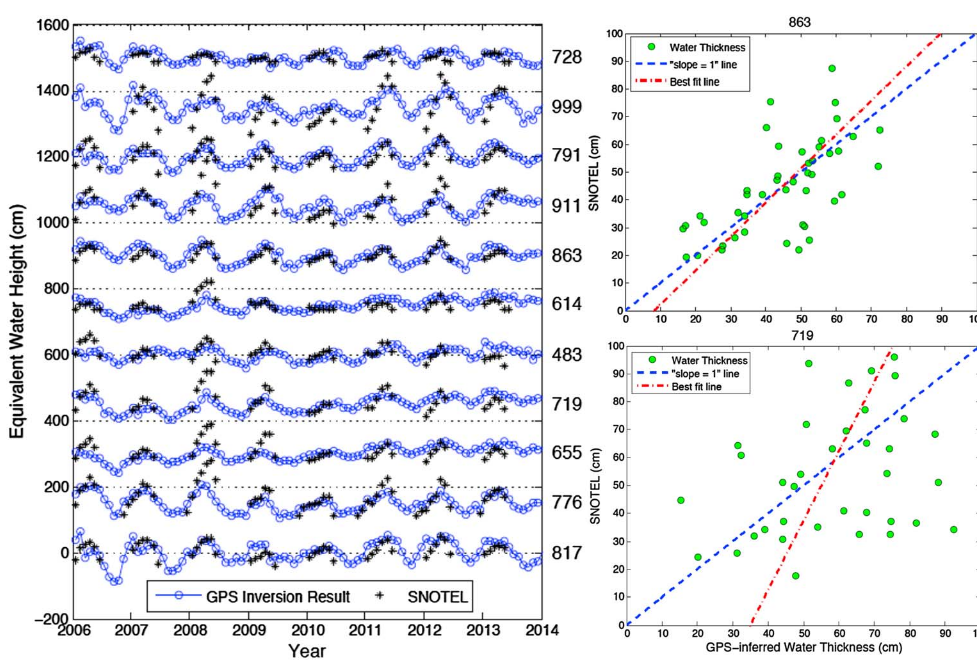

Figure 10. (left) Comparison between in situ SNOTEL measurement (http://www.wcc.nrcs.usda.gov/snow/) and GPS-inferred surface mass variations in Equivalent Water Height. (right) Detailed comparison of monthly water thickness for example SNOTEL sites 863 and 719. "Slope = 1" (blue dashed) line represents an ideal case that GPS and SNOTEL perfectly match each other. The red dash-dotted line is the best fit using the weighted total least squares method.

Figure 10 (right) plots detailed comparisons of monthly water thickness for SNOTEL site 863 (White Pass, Washington) with good agreement between GPS and SNOTEL and site 719 (Roaring River, Oregon) with poor correlation. If GPS and SNOTEL perfectly matched each other, all data points should align along the "Slope = 1" (blue dashed) line. The red dash-dotted line is the best fit using the weighted total least squares method. The correlation coefficient between GPS and SNOTEL is 0.63 for SNOTEL site 863 and 0.28 for site 719, and the average correlation coefficient for all the sites used in this study is 0.43 ± 0.13. Actually, we cannot expect "perfect" agreements between GPS-inferred and SNOTEL-observed mass variation, because SNOTEL is an observation at a point and depends strongly on local topography whereas GPS inversion smoothes the surface mass changes due to limited observations, and therefore, some detailed information within a local small region may be partly smeared out or not properly resolved (see discussion section for synthetic tests). Additionally, surface mass changes as recorded by GPS include soil moisture component not recorded by SNOTEL.

4. Discussion

4.1. Why Use GPS-Derived Water Variation?

Compared with GRACE observed water variations, GPS has some unique advantages. For the areas with dense GPS networks, GPS provides terrestrial water mass changes with higher spatial resolution than GRACE. In addition, the current GRACE data processing standard implies 2–3 months of data latency for GRACE monthly solutions. In contrast, GPS position series has the potential to be in near real time. For example, with rapid orbit and clock products, GPS positions can be derived with only 1 day latency, allowing much quicker estimation of the water storage changes compared with GRACE. Additionally, we have shown that GPS-inferred hydrological water variations can determine the scaling factors for GRACE measurement, and can also fill the current and future temporal gaps when GRACE observations might not available. Those are some unique advantages of GPS water solution. However, the method demonstrated in this paper requires a dense GPS network, because detailed water load features may not be recovered for the areas without GPS measurements.

4.2. Synthetic Tests of Inversion Method

Bevis et al. [2005] found that GPS vertical elastic response is dominated by loads with a horizontal scale of ~10^2 km. To determine how large an area should be included in our inversion, and we extend the region where we invert for surface mass variations to the north, east, and south (note west is the Pacific Ocean). The area of Washington and Oregon covers about 42°N–49°N, Pacific coast-117°W. We first set up our inversion area as 41.5°N–49.5°N, Pacific coast-116.5°W, and extended this area 1° to the north, south, and east, 40.5°N–50.5°N, Pacific coast-115.5°W, and invert for surface mass change. Then we do similar tests with the inversion region extended 2° (39.5°N–51.5°N, Pacific coast-114.5°W) and 3° (38.5°N–52.5°N, Pacific coast-113.5°W), individually. We find that the GPS-inferred surface masses change at the edge region of Washington and Oregon when we extend the area for inversion. This "edge" effect cannot be ignored. GPS-inferred mass at the edge region of Washington and Oregon may change by up to ~20% if we extend our domain by 1°. The differences decrease to ~9% between the solutions of inferred domain extended from 1° to 2°. The difference is less than 2% between solutions of inferred domain extended from 2° to 3°. The fact that the difference between results of extending 2° and 3° is so small means that extending inversion area 2.5° larger than Washington and Oregon is sufficient for the purpose of this study.

In order to verify the sensitivity and robustness of our inversion approach, we conduct a series of synthetic tests. We compute the loading deformation at GPS stations based on synthetic models of seasonal water load distribution and then invert the synthetic GPS data for surface mass distribution. Figures 11a and 11b show the result of a synthetic checkerboard test. The inversion (Figure 11b) recovers the input model (Figure 11a) well for the western part of these two states where more GPS stations are located. We also conduct a synthetic test using the seasonal change of our composite hydrology model (soil moisture from NLDAS plus snow data from SNODAS) as a input model (Figure 11c), calculate its resulting seasonal deformation at GPS locations, and invert for surface water variations using these synthetic GPS data (Figure 11d). These tests indicate that our inversion can recover the input model well for the western part of Washington and Oregon where GPS stations are denser. Figure S2 (supporting information) plots

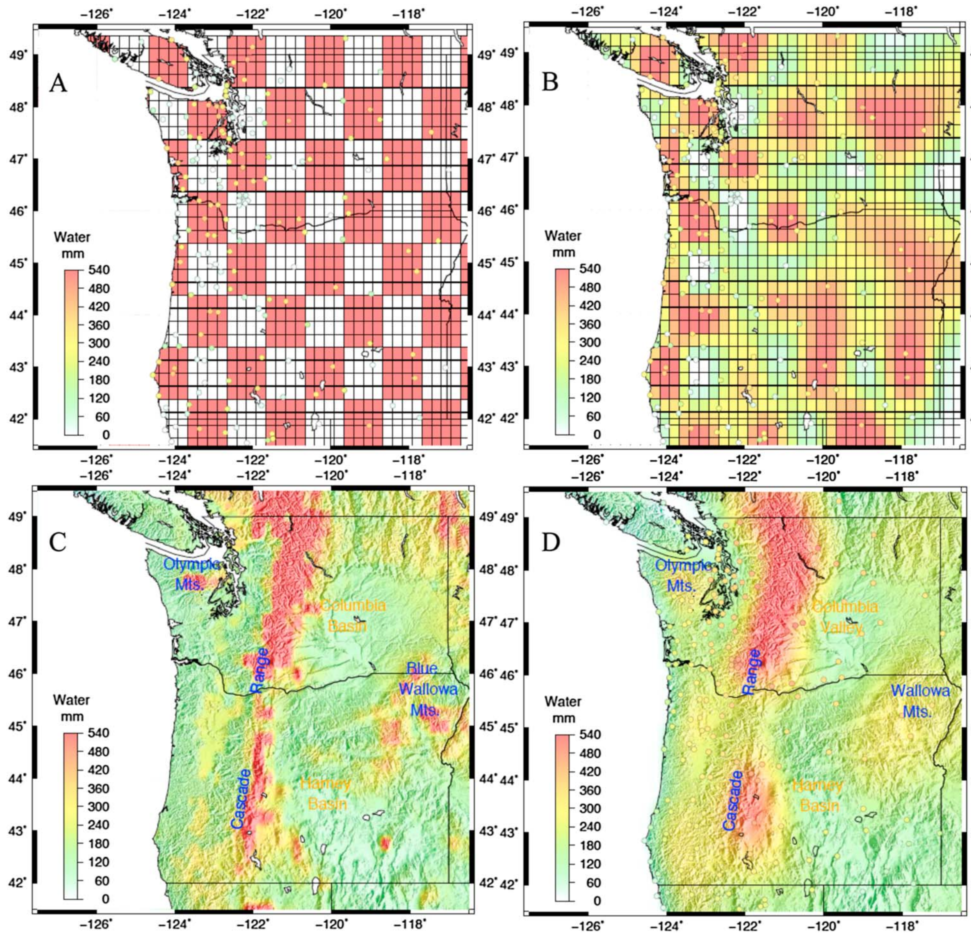

Figure 11. Results of synthetic tests. (a and b) For a checkerboard test. Inversion result (Figure 11b) is from the synthetic GPS data (circles) based on a checkerboard model (Figure 11a). (c and d) For a test using our composite hydrology model. Figure 11d is the inversion result of the composite model Figure 11c.

the ratio of input hydrology composite model (Figure 11c) to GPS inversion result (Figure 11d). Due to the sparse GPS distribution, some detailed features may not be recovered in the eastern part of these two states. In order to augment GPS hydrological loading research, more continuous GPS stations are needed in the eastern part of Washington and Oregon to improve the observational network.

We also perform a synthetic test using the time-variable terrestrial water mass change from our composite hydrology model as the input. We first calculate the loading deformation time series of GPS stations for the time periods when the stations are operational. This means our synthetic GPS time series have the same observational periods as the real GPS measurements. Then we invert the synthetic GPS monthly time series for terrestrial water mass change, and compare with the composite model. Figure 12 plots the comparison results for the Cascade Range and indicates that the inversion can recover the history of surface mass change. The maximum difference between the "true" input model and GPS-inferred result is only 5–8% of the true annual peak-to-peak surface mass change. Those differences occurred during the periods of large surface mass load (fall and winter seasons), with the GPS-inferred surface mass underestimating the composite truth model during this period. Those facts demonstrate that the inversion can recover most of the near-surface mass change, and only $<8\%$ signals may be smoothed out of the Cascade Range by the inversion process.

To make our inversion results stable, we apply the Laplacian smoothing constraints between neighboring grids during the inversion. The roughness weight β, which adjusts the relative importance between data fit and smoothness, is selected based on the trade-off curve between misfit and roughness (Figure 13). We evaluate a group of smoothing factors β and choose $\beta = 3$ as our optimal roughness weight because it can generate both reasonable data fits and roughness; see Figure 13. A smaller smoothing factor may

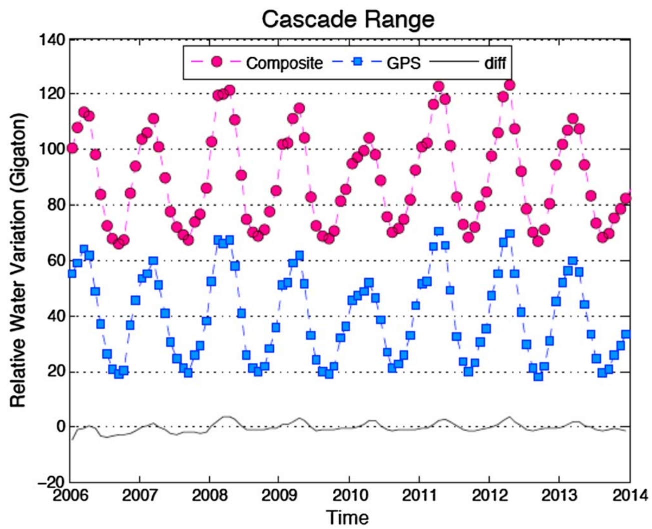

Figure 12. Synthetic test results using the time-variable terrestrial water mass change from our composite hydrology model as the input. This figure shows the comparison of water mass variations between the composite model (red circles, soil moisture of NLDAS plus snow data from SNODAS) and the GPS-inferred results (blue squares) with synthetic GPS data.

introduce rapid and unphysical spatial variation of inferred water distribution, and larger factors may lead to poor fit between observation and model.

4.3. Potential Errors in GPS Time Series

Spurious low frequency signals have been realized in GPS time series [e.g., *Penna et al.*, 2007; *King et al.*, 2008; *Tregoning and Watson*, 2009]. Particularly, *Ray et al.* [2008] highlights a systematic error associated with the draconitic period of 351.2 days, which is close to the solar annual period. In order to check the influence of this potential systematic error, we analyze JPL's eprocessed GPS time series [*Desai et al.*, 2011] used in this study. A stacked power spectrum analysis for all the continuous GPS series used in this study shows that after removing annual and semiannual fits, although the draconitic period does not clearly appear, the second and third draconitic harmonics are still there in the power spectrum, which is an indication of the draconitic component in GPS time series (Figure S3a, supporting information). To further investigate the effect of the draconitic component, we selected a group of continuous GPS station in Washington and Oregon with measurements longer than 13 years. The power spectrum analysis (Figure S3b in the supporting information) indicates similar features for the second and third draconitic harmonics. In order to quantify the potential systemic errors due to the draconitic component, we fit GPS time series with annual, semiannual, draconitic (and second draconitic) components simultaneously for the stations with observations longer than 13 years. Figure S3c plots the time series and its fit for station DRAO. DRAO is the continuous station with longest observational span since 1994. The amplitude of the draconitic component is 0.03 cm, and the amplitude of annual component is 0.48 cm. The amplitude of the second draconitic component is 0.01 cm compared with 0.15 cm of the semiannual component. If we fit annual, semiannual, draconitic, and second draconitic terms for the selected stations with measurement longer than 13 years (13 years of measurements are enough to distinguish the second draconitic harmonic component and semiannual period, and at least 25 years of observations are required to separate the draconitic component and annual period), the mean ratio between the amplitudes of draconitic component and the amplitudes of annual component is 21.13% ± 13.67%. The mean ratio between the amplitude of the second draconitic harmonic component and the amplitude of semiannual component is 22.52% ± 15.78%. If we only include the draconitic term, the mean ratio between the amplitudes of the

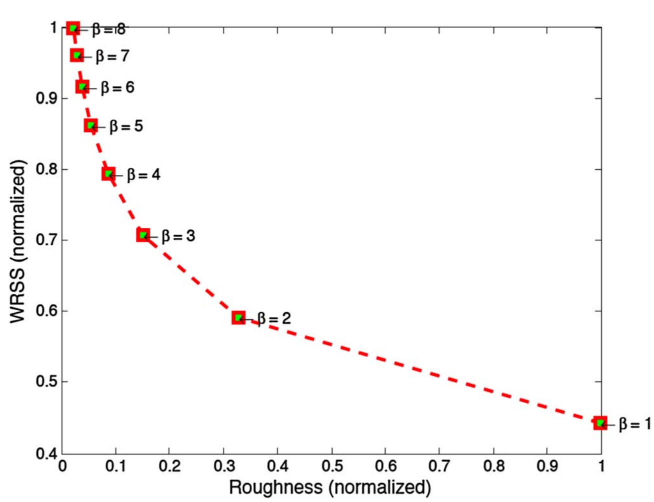

Figure 13. Trade-off curve between data fit (WRSS, Weighted-Residual Sum of Squares) and Roughness. WRSS and Roughness are normalized by dividing by their individual maximum value.

draconitic component and the amplitude of annual component is 21.24% ± 13.56%. Thus, we think the draconitic component is a potential systematic error in GPS time series, which may affect the accuracy of GPS's application for hydrological study. A recent study [*Rodriguez-Solano et al.*, 2014] shows that part of the draconitic errors in GPS series are induced by the radiation pressure orbit modeling deficiencies.

Periodic Slow Slip Events (SSE) within the Cascadia subduction zone usually have a regular period of 13–16 months [*Rogers and Dragert*, 2003], but they are mainly observed in the GPS horizontal component. Our study only uses GPS vertical displacements to estimate surface water loading distribution, so our results should not be affected by the tectonic SSEs. Further loading research that includes GPS horizontal measurements may need to take SSEs effects into consideration.

5. Conclusion

Our study demonstrates that a dense continuous GPS network is capable of providing quantitative estimates of terrestrial water storage variations by inverting the GPS-based surface deformation observations. In Washington and Oregon, most water variability is located within the mountain regions, whereas the water load is relatively small in the valleys and basins. As an independent measurement, water storage estimated from GPS-measured surface loading deformation is uniquely complementary to GRACE time-variable gravity measurements and hydrological models for assessing water resources. To improve the accuracy of GPS vertical deformation measurements for hydrological and other geophysical applications, further improvements in the data processing to reduce the draconitic systematic error in GPS series will increase the accuracy of GPS-inferred water storage changes.

GPS-inferred terrestrial water mass variation can be used to fill the temporal gap between current GRACE mission and future GRACE Follow-on mission, and to determine scaling factors for GRACE solutions. Therefore, near real-time GPS surface deformations can provide a more complete and accurate picture of regional water storage changes, and benefit water resource management and policies. The strategy of estimating time-variable water storage variations used in this paper for Washington and Oregon requires a dense continuous GPS network, or detailed features may not be recovered. Therefore, the discussed method can be applied to other places with dense GPS networks, such as Japan [*Heki*, 2004], Europe [*van Dam et al.*, 2007], and California [*Argus et al.*, 2014].

Acknowledgments
We greatly appreciate Christopher Watson, Tonie van Dam, and the editor Paul Tregoning for constructive comments that significantly helped to improve the manuscript. Y.F. thanks Richard Gross and Michael Watkins for helpful discussions. We are grateful to JPL's GPS data processing group, A. Moore, S. Owen, M. Heflin, S. Desai, W. Bertiger, and other members, and the UNAVCO, NSF Plate Boundary Observatory, and NASA MEaSUREs projects for GPS observations and data organization. All the data and results derived in this study are available from the authors. Y.F. is supported through the NASA Postdoctoral Program at Jet Propulsion Laboratory. The research described in this paper was carried out at the Jet Propulsion Laboratory, California Institute of Technology, sponsored by the National Aeronautics and Space Administration (NASA).

References

Amos, C. B., P. Audet, W. C. Hammond, R. Burgmann, I. A. Johanson, and G. Blewitt (2014), Uplift and seismicity driven groundwater depletion in central California, *Nature*, doi:10.1038/nature13275.

Argus, D. F., Y. Fu, and F. W. Landerer (2014), Seasonal variation in total water storage in California inferred from GPS observations of vertical motion, *Geophys. Res. Lett.*, *41*, 1971–1980, doi:10.1002/2014GL059570.

Bevis, M., D. Alsdorf, E. Kendrick, L. P. Fortes, B. Forsberg, R. Smalley Jr., and J. Becker (2005), Seasonal fluctuations in the mass of the Amazon River system and Earth's elastic response, *Geophys. Res. Lett.*, *32*, L16308, doi:10.1029/2005GL023491.

Blewitt, G., D. Lavallée, P. Clarke, and K. Nurudinov (2001), A new global model of Earth deformation: Seasonal cycle detected, *Science*, *294*, 2342–2345, doi:10.1126/science.1065328.

Boehm, J., B. Werl, and H. Schuh (2006), Troposphere mapping functions for GPS and very long baseline interferometry from European Centre for Medium-Range Weather Forecasts operational analysis data, *J. Geophys. Res.*, *111*, B02406, doi:10.1029/2005JB003629.

Borsa, A. A., D. C. Agnew, and D. R. Cayan (2014), Ongoing drought-induced uplift in the western United States, *Science*, *345*, doi:10.1126/science.1260279.

Chanard, K., J. P. Avouac, G. Ramillien, and J. Genrich (2014), Modeling deformation induced by seasonal variations of continental water in the Himalaya region: Sensitivity to Earth elastic structure, *J. Geophys. Res. Solid Earth*, *119*, 5097–5113, doi:10.1002/2013JB010451.

Chew, C. C., and E. E. Small (2014), Terrestrial water storage response to the 2012 drought estimated from GPS vertical position anomalies, *Geophys. Res. Lett.*, *41*, 6145–6151, doi:10.1002/2014GL061206.

Desai, S. D., W. Bertiger, B. Haines, N. Harvey, C. Sella, A. Sibthorpe, and J. P. Weiss (2011), Results from the reanalysis of global GPS data in the IGS08 reference frame, Abstract G53B-0904 presented at 2011 Fall Meeting, AGU, San Francisco, Calif., 5–9 Dec.

Dziewonski, A., and D. L. Anderson (1981), Preliminary reference Earth model, *Phys. Earth Planet. Inter.*, *25*, 297–356.

Elliott, J. L., J. T. Freymueller, and B. Rabus (2007), Coseismic deformation of the 2002 Denali fault earthquake: Contributions from synthetic aperture radar range offsets, *J. Geophys. Res.*, *112*, B06421, doi:10.1029/2006JB004428.

Famiglietti, J. S., M. Lo, S. L. Ho, J. Bethune, K. J. Anderson, T. H. Syed, S. C. Swenson, C. R. de Linage, and M. Rodell (2011), Satellites measure recent rates of groundwater depletion in California's Central Valley, *Geophys. Res. Lett.*, *38*, L03403, doi:10.1029/2010GL046442.

Farrell, W. E. (1972), Deformation of the Earth by surface loads, *Rev. Geophys.*, *10*, 761–797, doi:10.1029/RG010i003p00761.

Fu, Y., and J. T. Freymueller (2012), Seasonal and long-term vertical deformation in the Nepal Himalaya constrained by GPS and GRACE measurements, *J. Geophys. Res.*, *117*, B03407, doi:10.1029/2011JB008925.

Fu, Y., and J. T. Freymueller (2013), Repeated large Slow Slip Events at the south central Alaska Subduction zone, *Earth Planet. Sci. Lett.*, *375*, 303–311, doi:10.1016/j.epsl.2013.05.049.

Fu, Y., J. T. Freymueller, and T. Jensen (2012a), Seasonal hydrological loading in southern Alaska observed by GPS and GRACE, *Geophys. Res. Lett.*, *39*, L15310, doi:10.1029/2012GL052453.

Fu, Y., J. T. Freymueller, and T. van Dam (2012b), The effect of using inconsistent ocean tidal loading models on GPS coordinate solutions, *J. Geod.*, *86*(6), 409–421, doi:10.1007/s00190-011-0528-1.

Fu, Y., D. F. Argus, J. T. Freymueller, and M. B. Heflin (2013), Horizontal motion in elastic response to seasonal loading of rain water in the Amazon Basin and monsoon water in Southeast Asia observed by GPS and inferred from GRACE, *Geophys. Res. Lett.*, *40*, 6048–6053, doi:10.1002/2013GL058093.

Grapenthin, R., F. Sigmundsson, H. Geirsson, T. Árnadóttir, and V. Pinel (2006), Icelandic rhythmics: Annual modulation of land elevation and plate spreading by snow load, *Geophys. Res. Lett.*, *33*, L24305, doi:10.1029/2006GL028081.

Gross, R. S., G. Blewitt, P. J. Clarke, and D. Lavallée (2004), Degree-2 harmonics of the Earth's mass load estimated from GPS and Earth rotation data, *Geophys. Res. Lett.*, *31*, L07601, doi:10.1029/2004GL019589.

Harris, R. A., and P. Segall (1987), Detection of a locked zone at depth on the Parkfield, California, segment of the San Andreas fault, *J. Geophys. Res.*, *92*(B8), 7945–7962, doi:10.1029/JB092iB08p07945.

Heki, K. (2004), Dense GPS array as a new sensor of seasonal changes of surface loads, in *The State of the Planet: Frontiers and Challenges in Geophysics, Geophys. Monogr. Ser.*, vol. 150, edited by R. S. J. Sparks and C. J. Hawkesworth, pp. 177–196, AGU, Washington, D. C., doi:10.1029/150GM15.

Houborg, R., M. Rodell, B. L. Li, R. Reichle, and B. F. Zaitchik (2012), Drought indicators based on model-assimilated Gravity Recovery and Climate Experiment (GRACE) terrestrial water storage observations, *Water Resour. Res.*, *48*, W07525, doi:10.1029/2011WR011291.

Hreinsdóttir, S., J. T. Freymueller, H. J. Fletcher, C. F. Larsen, and R. Bürgmann (2003), Coseismic slip distribution of the 2002 M_w7.9 Denali Fault earthquake, Alaska, determined from GPS measurements, *Geophys. Res. Lett.*, *30*(13), 1670, doi:10.1029/2003GL017447.

King, M. A., C. S. Watson, N. T. Penna, and P. J. Clarke (2008), Subdaily signals in GPS observations and their effect at semiannual and annual periods, *Geophys. Res. Lett.*, *35*, L03302, doi:10.1029/2007GL032252.

Kouba, J. (2008), Implementation and testing of the gridded Vienna Mapping Function 1 (VMF1), *J. Geod.*, *82*, 193–205, doi:10.1007/s00190-007-0170-0.

Landerer, F. W., and S. C. Swenson (2012), Accuracy of scaled GRACE terrestrial water storage estimates, *Water Resour. Res.*, *48*, W04531, doi:10.1029/2011WR011453.

Lyard, F., F. Lefevre, T. Letellier, and O. Francis (2006), Modelling the global ocean tides: Insights from FES2004, *Ocean Dyn.*, *56*, 394–415.

Mitchell, K. E., et al. (2004), The multi-institution North American Land Data Assimilation System (NLDAS): Utilizing multiple GCIP products and partners in a continental distributed hydrological modeling system, *J. Geophys. Res.*, *109*, D07S90, doi:10.1029/2003JD003823.

National Operational Hydrologic Remote Sensing Center (2004), Snow Data Assimilation System (SNODAS) Data Products at NSIDC, Boulder, Colo. Natl. Snow and Ice Data Cent., doi:10.7265/N5TB14TC.

Ouellette, K. J., C. de Linage, and J. S. Famiglietti (2013), Estimating snow water equivalent from GPS vertical site-position observations in the western United States, *Water Resour. Res.*, *49*, 2508–2518, doi:10.1002/wrcr.20173.

Penna, N. T., M. A. King, and M. P. Stewart (2007), GPS height time series: Short-period origins of spurious long-period signals, *J. Geophys. Res.*, *112*, B02402, doi:10.1029/2005JB004047.

Price, E. J., and R. Bürgmann (2002), Interactions between the Landers and Hector Mine, California, earthquakes from space geodesy, boundary element modeling and time-dependent friction, *Bull. Seismol. Soc. Am.*, *92*(4), 1450–1469.

Ray, J., Z. Altamimi, X. Collieux, and T. van Dam (2008), Anomalous harmonics in the spectra of GPS position estimates, *GPS Solut.*, *12*, 55–64, doi:10.1007/s10291-007-0067-7.

Rodell, M., et al. (2004), The global land data assimilation system, *Bull. Am. Meteorol. Soc.*, *85*, 381–394.

Rodriguez-Solano, C. J., U. Hugentobler, P. Steigenberger, M. Blobfeld, and M. Fritsche (2014), Reducing the draconitic errors in GNSS geodetic products, *J. Geod.*, *88*, 559–574, doi:10.1007/s00190-014-0704-1.

Rogers, G., and H. Dragert (2003), Episodic tremor and slip on the Cascadia subduction zone: The chatter of silent slip, *Science*, *300*, 1942–1943, doi:10.1126/science.1084783.

Schmid, R., P. Steigenberger, G. Gendt, M. Ge, and M. Rothacher (2007), Generation of a consistent absolute phase center correction model for GPS receiver and satellite antennas, *J. Geod.*, *81*, 781–798, doi:10.1007/s00190-007-0148-y.

Sibthorpe, A., J. P. Weiss, N. Harvey, D. Kuang, and Y. Bar-Sever (2010), Empirical modeling of solar radiation pressure forces affecting GPS satellites, Abstract G54A-04 presented at 2010 Fall Meeting, AGU, San Francisco, Calif., 13–17 Dec.

Stark, P. B., and R. L. Parker (1995), Bounded-variable least-squares: An algorithm and application, *Comput. Stat.*, *10*(2), 129–141.

Swenson, S. C., and J. Wahr (2006), Post-processing removal of correlated errors in GRACE data, *Geophys. Res. Lett.*, *33*, L08402, doi:10.1029/2005GL025285.

Tapley, B. D., S. Bettadpur, M. M. Watkins, and C. Reigber (2004), The Gravity Recovery and Climate Experiment: Mission overview and early results, *Geophys. Res. Lett.*, *31*, L09607, doi:10.1029/2004GL019920.

Tregoning, P., and C. Watson (2009), Atmospheric effects and spurious signals in GPS analyses, *J. Geophys. Res.*, *114*, B09403, doi:10.1029/2009JB006344.

Tregoning, P., C. Watson, G. Ramillien, H. McQueen, and J. Zhang (2009), Detecting hydrologic deformation using GRACE and GPS, *Geophys. Res. Lett.*, *36*, L15401, doi:10.1029/2009GL038718.

van Dam, T. (2010), NCEP Derived 6 hourly, global surface displacements at 2.5 × 2.5 degree spacing. [Available at http://geophy.uni.lu/ncep-loading.html.]

van Dam, T. M., and J. M. Wahr (1987), Displacements of the Earth's surface due to atmospheric loading: Effects on gravity and baseline measurements, *J. Geophys. Res.*, *92*, 1281–1286, doi:10.1029/JB092iB02p01281.

van Dam, T., J. Wahr, and D. Lavallée (2007), A comparison of annual vertical crustal displacements from GPS and Gravity Recovery and Climate Experiment (GRACE) over Europe, *J. Geophys. Res.*, *112*, B03404, doi:10.1029/2006JB004335.

Wahr, J., S. A. Khan, T. van Dam, L. Liu, J. H. van Angelen, M. R. van den Broeke, and C. M. Meertens (2013), The use of GPS horizontals for loading studies, with applications to Northern California and southeast Greenland, *J. Geophys. Res. Solid Earth*, *118*, 1795–1806, doi:10.1002/jgrb.50104.

Wang, H., L. Xiang, L. Jia, L. Jiang, Z. Wang, B. Hu, and P. Gao (2012), Load Love numbers and Green's functions for elastic Earth models PREM, iasp91, ak135, and modified models with refined crustal structure from Crust 2.0, *Comp. Geosci.*, *49*, 190–199.

Wu, X., M. B. Heflin, E. R. Ivins, D. F. Argus, and F. H. Webb (2003), Large-scale global surface mass variations inferred from GPS measurements of load-induced deformation, *Geophys. Res. Lett.*, *30*(14), 1742, doi:10.1029/2003GL017546.

Zaitchik, B. F., M. Rodell, and R. H. Reichle (2008), Assimilation of GRACE terrestrial water storage data into a land surface model: Results for the Mississippi River Basin, *J. Hydrometeorol.*, *9*, 535–548, doi:10.1175/2007JHM951.1.

Zumberge, J. F., M. B. Heflin, D. C. Jefferson, M. M. Watkins, and J. F. H. Webb (1997), Precise point positioning for the efficient and robust analysis of GPS data from large networks, *J. Geophys. Res.*, *102*, 5005–5017, doi:10.1029/96JB03860.